

Dense outer layers formed by plasma treatments of silica coatings produced by the sol–gel method

L. MASCIA, Z. ZHANG

Institute of Polymer Technology and Materials Engineering, Loughborough University of Technology, Loughborough, Leicestershire LE11 3TU, UK

Silica gel coatings prepared by the sol–gel method were subjected to low-temperature plasma treatments in air and argon. This was found to give rise to the formation of a dense outer layer, whose thickness increased with the duration of the treatment and decreased when the pressure in the plasma chamber was reduced. The formation of a dense layer in the coatings was confirmed from measurements of the overall thickness and the refractive index by ellipsometry, and also from TEM examination and light transmission experiments. The coatings were found to contain an uppermost layer of alumina, which was formed through secondary sputtering of aluminium from the electrodes in the plasma chamber. The concentration of alumina in the mixture with silica decreased through the thickness of the coating and became zero at a distance slightly smaller than the overall thickness of the dense layer. The thickness of the dense layer was found to be slightly higher with argon than with air plasma treatments. Whereas the aluminium concentration through the thickness of the coating was the same for the two types of treatment, a carbon residue was found only in the case of argon plasma treatments. The composition of the underlying silica layers was found to correspond to $\text{SiO}_{1.6}$.

1. Introduction

In the preparation of glasses and ceramics by the sol–gel method, it is essential to convert the xerogel to a dense solid in order to develop adequate mechanical properties. As this has to be carried out by sintering at very high temperatures, the process imposes severe restrictions on the range of possible applications and precludes their use as coatings for organic polymers and in the fabrications of electronic devices. It is highly desirable, therefore, to find a “low-temperature” process for the sintering of metal oxide coatings produced by the sol–gel process.

Considering the problem in simple energetic terms, it is possible to foresee a solution with the use of low-temperature plasma. This concept has been explored, in fact, for the densification of compacted metal powders by means of laser-generated shock-waves which produce a high-pressure plasma against the surface of a metallic film placed over the target [1]. Glow-discharge plasma is also known to emit levels of energy sufficiently high to anodize thin films of silicon and various other metals to their oxide state [2].

The possibility of producing dense layers on sol–gel silica coatings has also been demonstrated using a plasma etcher at 130 kHz at 400 W and 6 Pa pressure [3, 4]. Similar types of dense layers, albeit considerably thinner, have been reported by the present authors with the use of a plasma etcher at substantially higher pressures [5]. In the latter case, the authors have shown that the thickness of the dense

layer decreases very rapidly with pressure and it extrapolates to zero for pressures just below atmospheric pressure. Treatments of sol–gel coatings with corona discharges, which operate at atmospheric pressure, were also found to be ineffective for the formation of a dense layer [5].

Because the rate of collision of glow-discharge ionized gas with the target surface is a predominate factor in plasma processing, it is feasible that the transfer of momentum associated with such a collision could raise the surface temperature at a rate which will allow it to reach the levels required to induce the collapse of the pores by viscous flow. The findings reported earlier suggest that these levels of energy are not reached if the pressure is too high, owing to the dissipation of the available energy in the gas phase through particle collisions before they reach the target surface.

This work was carried out, therefore, to elucidate the mechanism of the formation of the dense layer in silica coatings deposited by the sol–gel and to determine its chemical and physical characteristics.

2. Experimental procedure

2.1. Coatings preparation

A 44 wt % solution of tetraethoxysilane (TEOS) (98% purity grade from Janssen Chimica) in an ethanol/water mixture (1:11.6 molar ratio) was prepared and the

equivalent of 5 mol % HCl, with respect to the TEOS content, was added from a 32 wt % solution in water. The solution was shaken and kept at room temperature for 24 h under quiescent conditions to produce a hydrolysed "master" solution (sol). This was subsequently diluted with ethanol to produce several coating solutions, with equivalent TEOS concentrations varying from 0.9–7 wt %, in order to obtain a wide range of coating thicknesses covering in the range 25–100 nm.

Various materials were used as substrate, including biaxially oriented polyethylene terephthalate (PET) film (130 μm), microscope glass slides (1.2 mm thick), polished $\langle 100 \rangle$ single-crystal silicon wafers (530 μm thick) and aluminium foils (12 μm). In each case the coating was deposited on the substrate by a simple one-pass dip into the coating solution. The glass slides and silicon wafers were first degreased in ethanol, while the PET film was treated with air plasma for 5 min in a 50 cm diameter barrel type etcher (System 80 apparatus manufactured by Plasma Technology) with a power of 500 W at 100 kHz. The coatings were dried and "gelled" for 2 days at room temperature and then treated with air plasma under different conditions, using the same equipment and the same power input as specified earlier for the pretreatment of the PET films.

A number of experiments were repeated using argon plasma.

2.2. Coatings characterization

The morphology of the coatings was examined by taking samples produced on the PET film substrate. The films were embedded in epoxy resin and then microtomed into very thin slices for cross-section observation by transmission electron microscopy (TEM), using a TEM-100 CX apparatus manufactured by Jeol Ltd. Cross-sections of the coatings on PET films were also examined by scanning electron microscopy (SEM) using cryogenically fractured specimens which were subsequently etched in concentrated HCl (70 wt %).

The sol-gel coatings were examined with respect to their light transmission properties using glass slides as substrate. A Hitachi U-2000 spectrophotometer was used with a scan speed at 200 nm min^{-1} and list interval of 5 nm from 400–700 nm. The results were recorded as percentage light transmission through the whole sample, i.e. coating and substrate.

The refractive index and thickness of the coatings were measured by ellipsometry at 632.8 nm with a 50° incident angle and 90° retardation using a NEW Gaertner L117 Production Ellipsometer operating with laser-polarized light.

The dehydration of the coatings caused by the plasma treatment was monitored by Fourier transform-infrared (FT-IR) measurements on samples supported on aluminium foils using the attenuated total reflectance (ATR) technique on a Mattson 300 spectrometer fitted with a Specac ATR attachment. The internal reflection element was a ZnS crystal and the incident angle was 45°. The samples

were examined with a resolution of 2 cm^{-1} at 1000 scans.

The total duration of the plasma treatment was accumulated in consecutive steps after each spectrometric examination.

The coatings composition through their thickness was analysed at CSMA Ltd using the depth-profile XPS technique on coatings supported on PET films. The instrument used for the analysis was a VG 220i Imaging XPS. Depth profiling was carried out with a 4.5 keV argon ion beam rastered on an area of approximately $2 \times 1.2 \text{ mm}^2$. The depth scale on the profile was obtained from calibration on tantalum oxide film, which gave an etch rate of 10.7 nm min^{-1} .

3. Results and discussion

3.1. Physical structure of plasma-treated silica gel coatings

Fig. 1 shows a typical transmission electron micrograph of a silica-gel coating after removing the solvent by evaporation. The micrograph reveals the typical density fluctuations associated with interconnected particles/pores morphology of xerogels. The interparticle surface-to-surface distance is 3–4 nm and the diameter of the particles (dark domains) is in the region of 2–3 nm.

After plasma treatment, a distinct dense layer is observed on the outer surface of the coating, which increases in thickness with increasing treatment time (Fig. 2). These transmission electron micrographs show that with prolonged treatments, it is possible to produce dense layers to considerable depths from the top surface, i.e. 50 nm or more. Stratified layers of dense material were also obtained by intermittent coating and plasma treatment operations (Fig. 2b).

The thickness of the dense layer as a function of treatment time is shown in Fig. 3. This plot reveals that the increase in thickness is not linear but sigmoidal, i.e. it bears some similarity to thermal sintering of powder coatings [6]. It is noted that argon plasma produces slightly thicker layers of dense matter in the coatings.

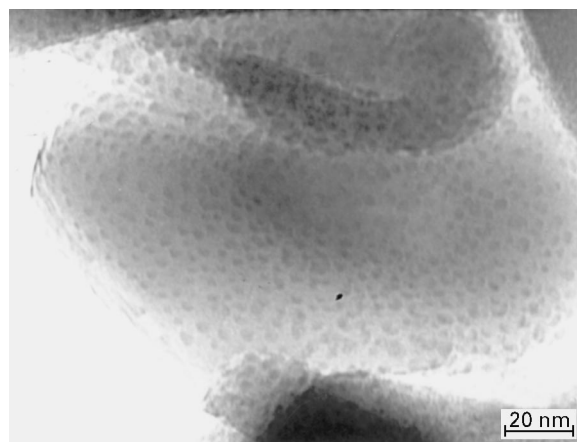


Figure 1 Transmission electron micrograph of pristine silica coatings deposited by the sol-gel method.

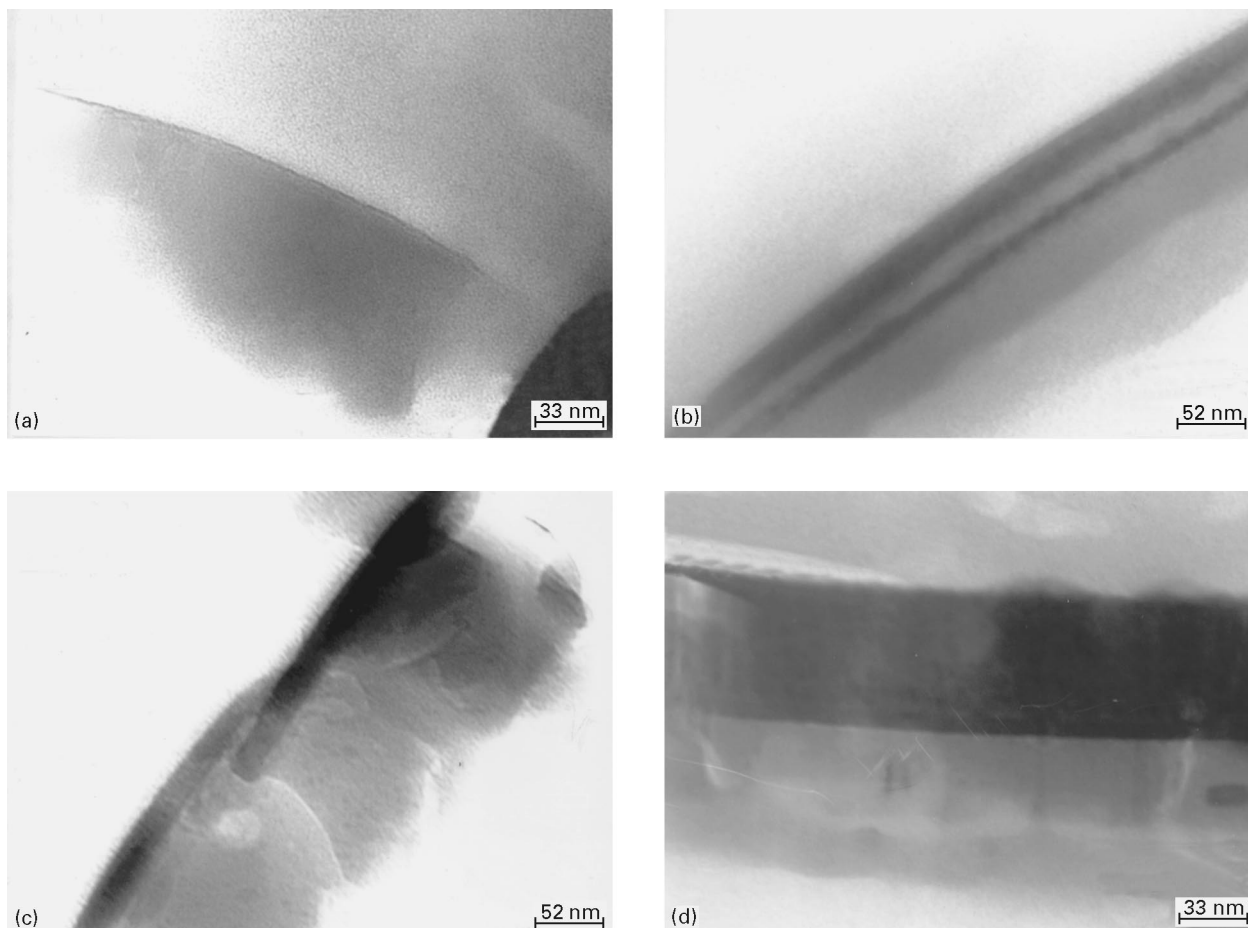


Figure 2 Transmission electron micrograph of silical coatings after air plasma treatments (500 W, 40 Pa pressure) for (a) 2 min, (b) upper layer 20 min, bottom layer 10 min, (c) 25 min, (d) 60 mins.

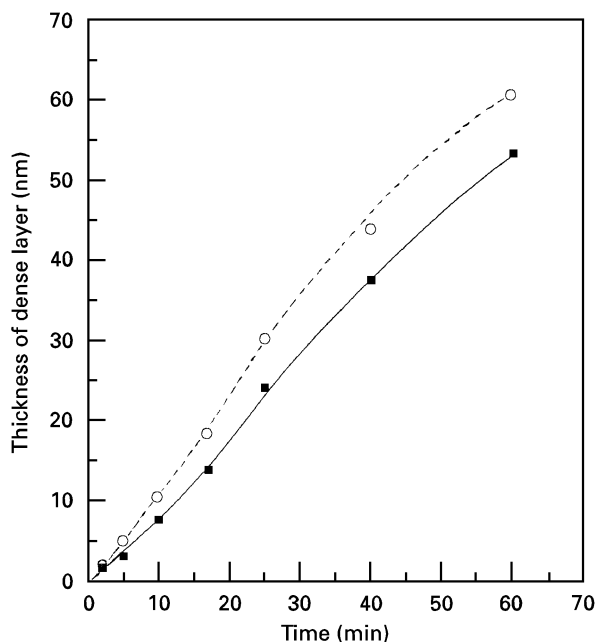


Figure 3 Thickness of the dense surface layer of air plasma-treated silica coatings as a function of treatment time (500 watts, 40Pa pressure): (■) air plasma, (○) argon plasma.

The evidence that the darker outer skin of the coating shown in Fig. 2 is a dense layer can also be obtained from an inspection of the scanning electron micrograph in Fig. 4, taken on a plasma-treated coat-

ing after immersing in concentrated HCl. A clearly visible top layer of less porous material is observed and appears to be delaminating from the sublayer.

3.2. Optical properties of plasma-treated silica gel coatings

Fig. 5 shows plots of the percentage light transmission against wavelength of the incident light for silica gel coatings on glass slide substrate. These reveal the well-known antireflective behaviour of xerogels [7, 8] associated with a reduction in refractive index in the outer layers. Treating the coatings with air plasma was found to cause a reduction in light transmission by an extent which depends on the duration of the treatment and the gas pressure. The quantitative relationships between light transmission of coated glass slides and plasma treatment time and gas pressure, respectively, are shown graphically in Figs 6 and 7.

The reduction in light transmission caused by the plasma treatment is a manifestation of the formation of a dense layer in the coatings, owing to the light transmission dependence of a coated substrate on the refractive index of the coatings, which is related to its density [9].

The relationship between density and refractive index can be described by the equation [10]

$$(n_p^2 - 1)/(n_d^2 - 1) = \rho_p/\rho_d \quad (1)$$

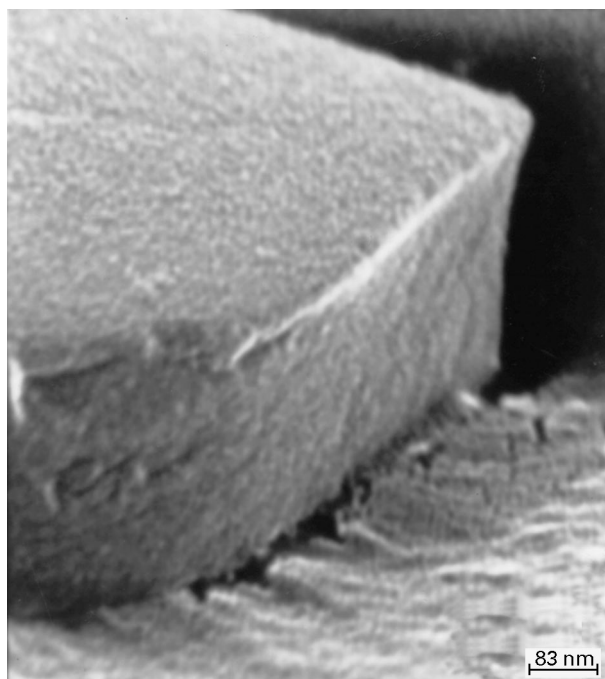


Figure 4 Scanning electron micrographs of cross-sections of silica coatings, treated with air plasma at 40 Pa and 500 W for 25 min and then etched with concentrated HCl acid for 5 min.

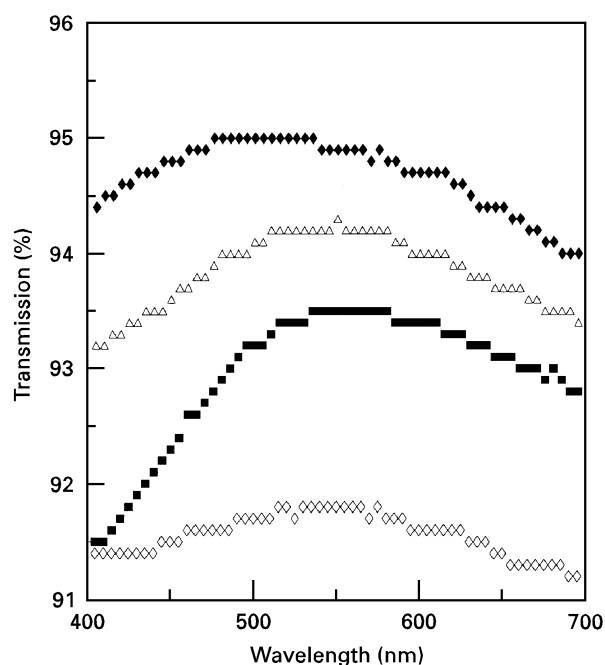


Figure 5 Light transmission of uncoated and silica-gel coated glass slides. (\diamond) Uncoated, (\blacklozenge) silica coated slides, before treatment; (\triangle) silica coated slides and treated with air plasma for 10 min; (\blacksquare) silica coated and treated with air plasma for 40 min. (Plasma processing conditions were 500 W and 40 Pa pressure.)

where n and ρ are refractive index and density, while the subscripts p and d denote, respectively, the porous and dense state of the material.

Fig. 8 shows a plot of refractive index of the coatings as a function of treatment time. In examining these data it is important to bear in mind that the original thickness of the coatings for each treatment time was chosen to correspond to the value taken as

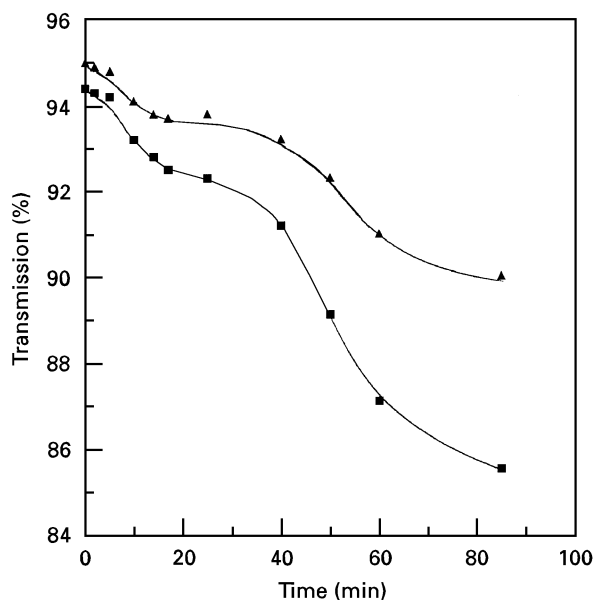


Figure 6 Light transmission of silica-coated glass slides as a function of air plasma-treatment time. (Plasma processing conditions were: 500 W and 40 Pa pressure.) Wavelength of incident light: (\blacksquare) 400 nm; (\blacktriangle) 500 nm.

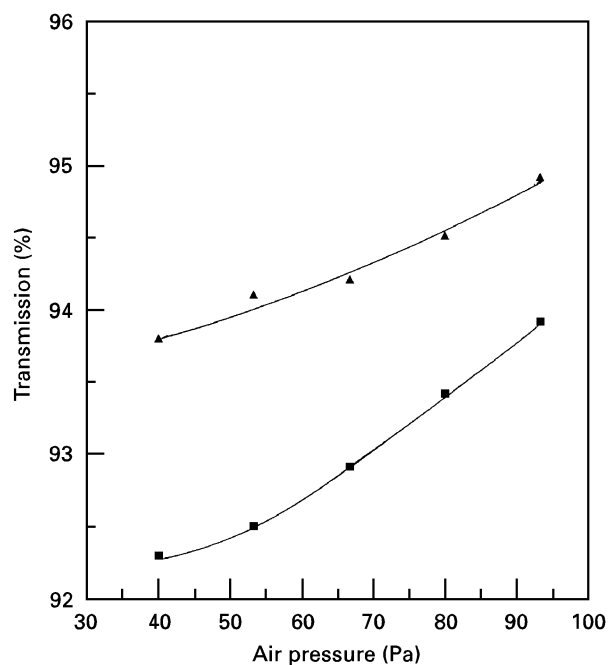


Figure 7 Light transmission of silica-coated glass as a function of air pressure used in the air plasma treatments. The samples were treated at 500 W for 25 min. Wavelength of incident light: (\blacksquare) 400 nm; (\blacktriangle) 500 nm.

the dense layer from the TEM examinations of plasma-treated coatings on the PET substrate, shown in Fig. 3. This procedure was adopted in order to eliminate the formation of two distinct layers with different refractive indices in the coatings, which would have interfered with the refractive index measurements.

If the only effect of the increase in plasma treatment time of the coatings was an increase in the thickness of the dense layer, the refractive index would have remained constant. It can be inferred, therefore, that the

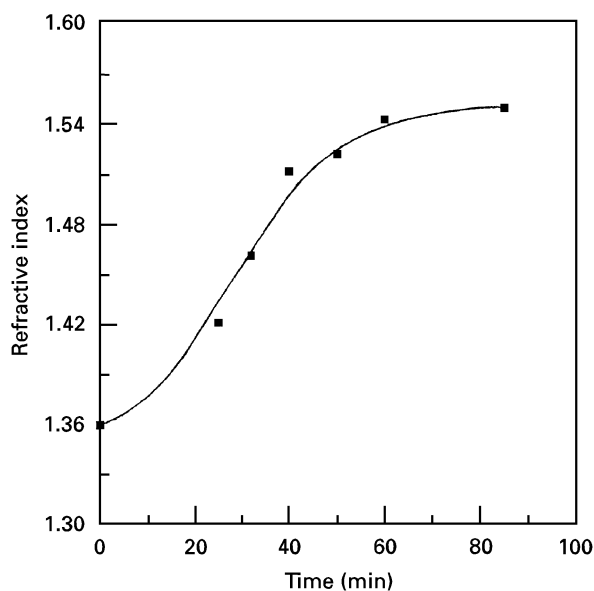


Figure 8 Refractive index of silica coatings on silicon wafers as a function of air plasma-treatment time. The samples were treated at 500 W and 40 Pa pressure.

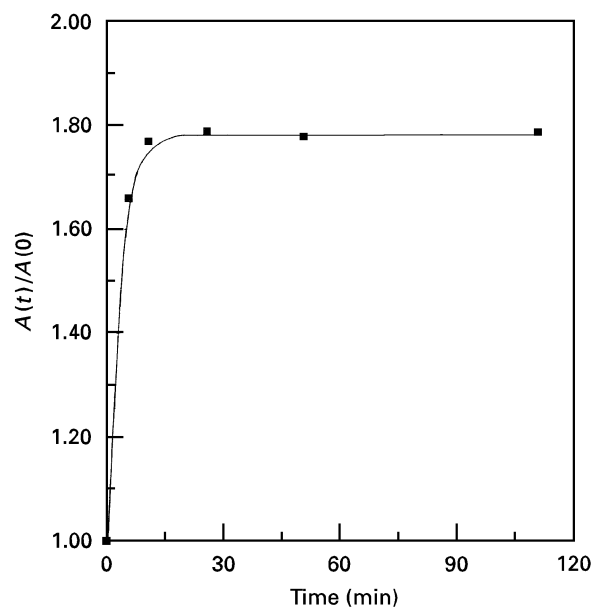


Figure 9 Relative FT-IR-ATR absorbance at 1056 cm^{-1} for silica coatings ($\sim 25\text{ nm}$ thick) as a function of air plasma-treatment time. (Air plasma processing conditions: 500 W and 40 Pa pressure.)

observed increase in refractive index with treatment time must have resulted from a further increase in the density of the coating unless there have been environmental interferences during the treatment to cause a simultaneous change in chemical composition through the incorporation of heavier atoms. In support of this hypothesis are the results of the FT-IR analysis which show that the absorbance at 1056 cm^{-1} , corresponding to the Si-O-Si asymmetric stretching vibration, does not undergo any further change with increasing treatment time, once the formation of a dense layer has been identified by TEM examination, i.e. after about 10 min for the treatment conditions used in this work. This is shown in Fig. 9 as a plot of the absorbance at 1056 cm^{-1} relative to that for the untreated sample, $A(t)/A(0)$, as a function of treatment time. These results confirm that the increase in refractive index after 25 min treatment time must be due to factors other than chemical changes in the structure of the sol-gel silica coating. The measured refractive index values of the coatings are, however, even greater than those obtained on thermally sintered coatings. The data in Fig. 8 show that the refractive index of the silica gel coatings reaches a plateau for values in the range of 1.54 after a prolonged plasma treatment, whereas a maximum value in the region of 1.46 is obtained for thermally sintered amorphous silicon dioxide [11, 12]. Plasma-induced crystallization phenomena for silica coatings have been reported in the literature [13, 14] and could be considered to be a contributing factor for the observed increase in refractive index.

Fig. 10a and b show the depth profiles of the coatings treated with air plasma, respectively, for 25 and 60 min. In both cases, a very thin layer of aluminium in the oxidized state, corresponding to Al_2O_3 , appears on the surface of the coating, while the atomic ratio of oxygen to silica increases through this layer, starting

from very low values at the surface and reaching a maximum value of 1.6 at the edge of the dense layer. This is not the case, on the other hand, for coatings treated with argon plasma, which were found to contain substantial quantities of carbon residues. The amount of carbon increased gradually through the thickness of the dense layer to a maximum concentration of about 20%. The depth profile of the carbon content for the two types of plasma treatments is shown in Fig. 11. The larger increase observed for argon treatments at depths greater than 100 nm corresponds to the surface of the PET substrate. This does not feature in the diagram corresponding to the coating treated with air plasma, owing to its thickness being appreciably greater than 100 nm. It is worth noting, however, that the aluminium concentration and the Si/O ratio through the thickness was found to be the same for the two types of treatments.

The oxidizing nature of the air plasma must be responsible for the complete expulsion of organic matter from the coating, which is expected to occur at a fairly early stage, i.e. before the formation of a dense layer. This has to take place through thermal oxidation as it is not expected that the ionized oxygen species would penetrate the pores of the xerogel through the entire thickness without losing their energy [15]. No explanation can be given for the low state of oxidation of the silica, other than a possible association with the reducing environment created by the residual organic matter from the TEOS.

It is noted that the concentration of aluminium decreases to zero at a distance slightly smaller than the thickness of the dense layer, particularly for argon plasma treatments, although this is not shown in Fig. 10b. The maximum concentration of aluminium, on the other hand, is found at a distance less than one-quarter of the thickness of the dense layer. The reduction in aluminium concentration on the outer

surface of the coatings is due to the presence of zinc and carbon contaminants (not shown in Fig. 10). These are likely to arise from the transfer of zinc stearate from the surface of the polyethylene sachet used for storing and transporting the samples. Metal stearates are widely used, in fact, as external lubricants in the manufacture of polymer films.

The presence of substantial amounts of aluminium through the thickness of the coatings, on the other hand, results from secondary sputtering depositions of aluminium oxide through erosion of the electrodes of the plasma barrel.

Because the refractive index of alumina is 1.62 it is possible that these deposits contribute substantially to the observed increase in refractive index of the coatings, but cannot be considered to be the sole cause on the basis of the arguments put forward earlier related

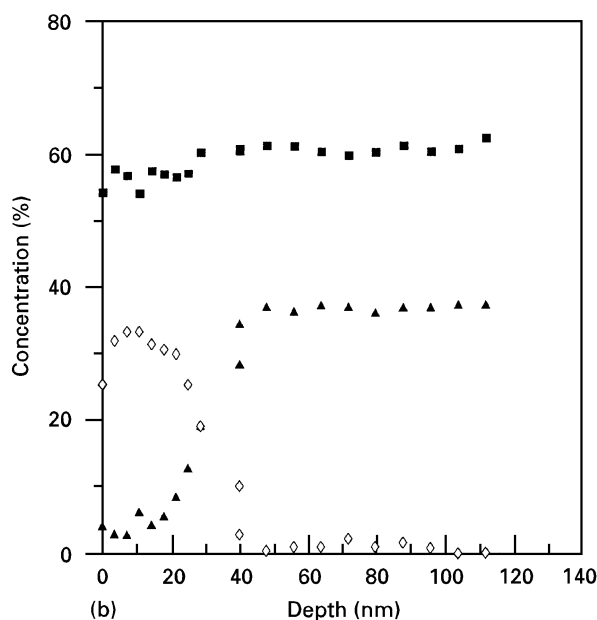
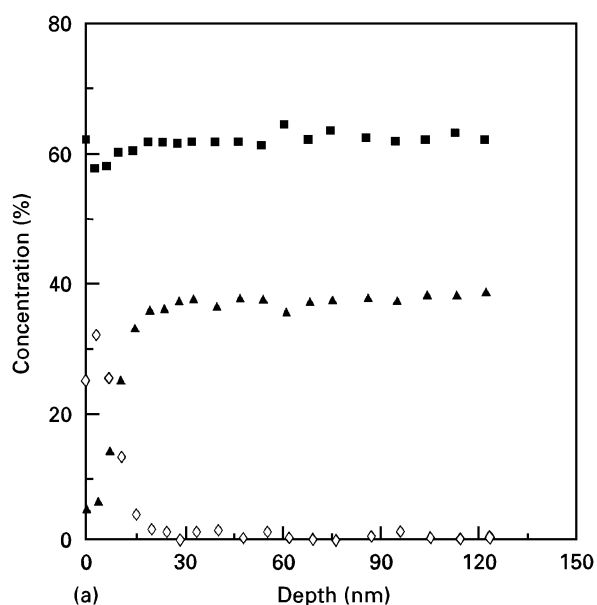


Figure 10 XPS depth profile of silica coatings after being treated with air plasma at 40 Pa pressure with a 500 W power input. (a) 25 min treatment, (■) O 1s, (▲) Si 2p, (◇) Al 2p. (b) 60 min treatment, (■) O 1s, (▲) Si 2p, (◇) Al 2p.

to the concentration distribution of aluminium through the thickness. Furthermore, one notes a substantial difference for the reduction in light transmission resulting from plasma treatments of silica-coated glass slides and that observed for non-coated glass slides subjected to the same treatments (see Fig. 12)

It may be assumed that the thickness of the sputtered alumina deposits was the same regardless of the nature of the substrate. Thus, the data in Fig. 12, showing a greater reduction in light transmission of the silica-coated glass slides, imply that changes have

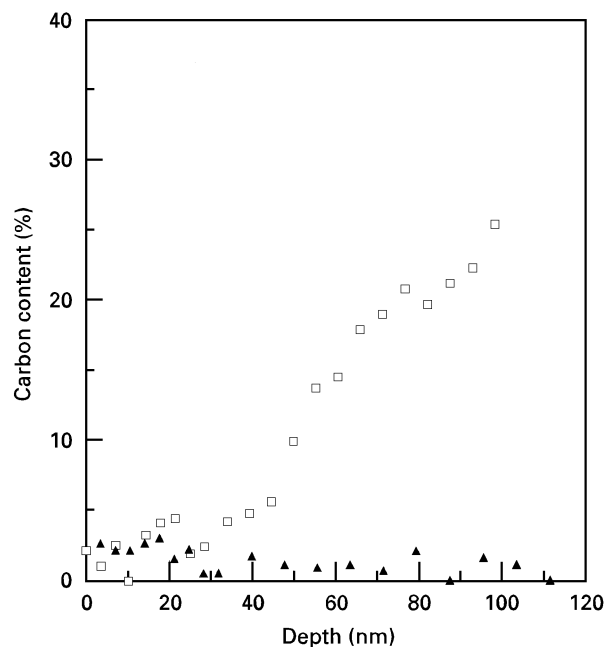


Figure 11 XPS depth profile of silica coatings after plasma treatments at 40 Pa pressure and 500 W for 60 min. (▲) Air plasma, (□) argon plasma.

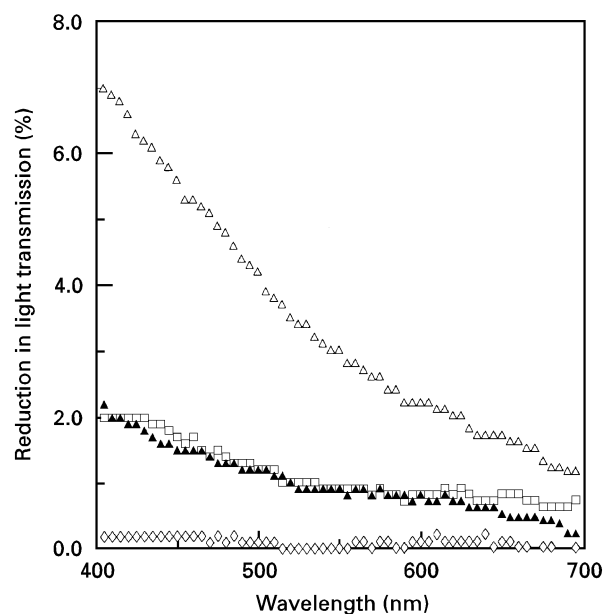


Figure 12 Reduction in light transmission of glass slides after air-plasma treatments at 40 Pa pressure with a 500 W power input. Silica coated glass slides: (□) 25 min and (△) 60 min plasma treatments. Non-coated glass slides: (◇) 25 min and (▲) 60 min plasma treatments.

occurred in the coatings rather than mere alumina deposition. For instance, at a wavelength of 400 nm of incident light, the reduction in light transmission resulting from 60 min plasma treatment is about 7% for the sol-gel coated glass slides and only 2% for the uncoated slides.

Because the refractive index, n , of SiO_x increases when the value of x decreases, a substantial contribution to the reduction in light transmission for the silica-coated samples may also be expected to derive from the $\text{SiO}_{1.6}$ composition of the silica coating. It is noted that at 550 nm wavelength of incident light, n is equal to 2.00 for $x = 1$, 1.52–1.55 for $x = 1.5$ and 1.46 for $x = 2$ [9]. Hence it is reasonable to presume that the refractive index of the plasma-treated coating could reach the value 1.54 at 632.8 nm (i.e. the wavelength of the light used for measuring the refractive index), irrespective of the presence of the alumina contamination on the surface.

The results of the thickness measurements of the coatings obtained by ellipsometry are particularly instructive for the elucidation of the morphology of plasma-treated coatings. These are plotted in Fig. 13 as the ratio of the original thickness value to that obtained after plasma treatment against the duration of the treatment. Despite the formation of a thin layer of alumina deposits on the surface and the increase in amounts of these with treatment time, the overall effect is a large reduction in the total thickness of the coating.

It is difficult, however, to make accurate calculations on the expected reduction in thickness which is expected to arise purely from the densification of silica, in view of the uncertainties due to variations in the initial thickness of the coatings and the density of SiO_x produced by the plasma treatment. Approximate estimates can be obtained by assuming that the density of

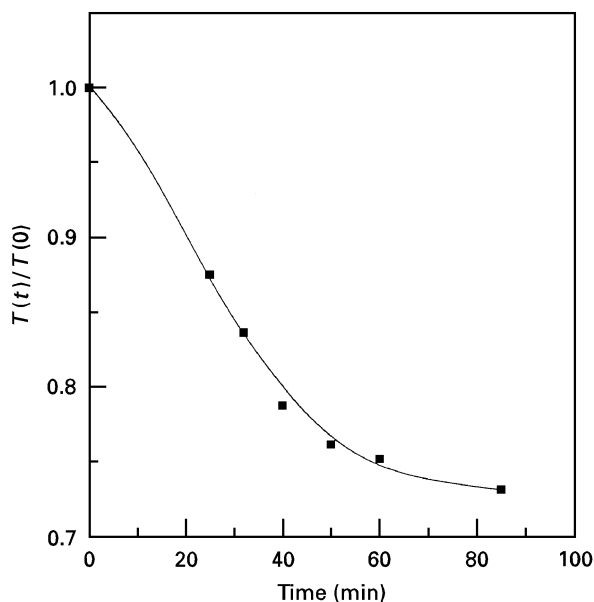


Figure 13 Normalized silica-coating thickness as a function of air plasma-treatment time. $T(t)$ = thickness at time t ; $T(0)$ = initial thickness. The coatings on silicon wafers were treated with air plasma at 40 Pa pressure and 500 W power input.

$\text{SiO}_{1.6}$ is not too different from that of amorphous SiO_2 . This implies that the density of the sintered layer of the coating increases approximately by a factor of 2 as a result of the plasma treatment. Under the usual plasma-treatment conditions, i.e. 40 Pa pressure and 400 W power input, a 60 min treatment is expected to produce a dense layer approximately 25 nm thick, based on an initial thickness in the region of 100 nm. In practice, this layer is found to be approximately 50 nm thick. The data in Fig. 10b show that there is a top layer of alumina 10 nm deep (including the contamination described earlier) and that the concentration of aluminium drops to zero at about 40–45 nm from the surface. From this it can be deduced that the total alumina content would correspond to a coating 25–30 nm thick.

The appearance of a sharp boundary at the interface between the dense upper layer and the undensified xerogel beneath is also an important parameter to consider in the interpretation of the results. It is clear that a simple layer-by-layer deposition mechanism for the accumulation of alumina on the surface, resulting from the plasma treatments, has to be excluded, owing to the existence of a concentration gradient and the observations related to the reduction in light transmission of coated glass slides relative to the uncoated samples.

The inverse concentration gradients for silica and alumina in the coatings suggest, on the other hand, that a diffusion process is operative during the earlier stages prior to the formation of a continuous layer of alumina. It is possible that small particles of alumina could penetrate fairly deeply into the porous xerogel through collisions, forming a dense layer consisting of a mixture of alumina and silica. Only after the formation of a hard layer is it possible for the alumina to accumulate and produce a homogeneous layer. The above mechanism would produce a blurred interphase at the boundary between densified material and undensified xerogel. It remains, therefore, that the only possible explanation for the occurrence of a sharp interface, between the dense layer and the porous xerogel layers beneath, is through melting and flow, i.e. thermal sintering. The extent to which this happens, however, is rather small and may be restricted to a few nanometres.

4. Conclusions

Although the occurrence of secondary sputtering depositions of alumina from the plasma chamber has not permitted indisputable evidence to be obtained for the formation of a dense layer by sintering through viscous flow, the study has brought to light some very important aspects of the interaction of plasma gases with silica coatings produced by the sol-gel method.

1. The initial stage of plasma treatments produce dehydration of silica gel coatings.
2. Total expulsion of carbonaceous matter is achieved by treatments with oxidizing plasma gases at low temperatures.

3. A silicon oxide structure equivalent to $\text{SiO}_{1.6}$ is formed regardless of the oxidizing power of the plasma gas used for the treatment.

4. A distinct dense layer is formed on the surface of the coatings, whose composition gradually changes from pure alumina at the outer surface to pure $\text{SiO}_{1.6}$ in the xerogel beneath.

References

1. D. ZAGOURI, J.-P. ROMAIN, B. DUBRUJEAUD and M. JEANDIN, *J. Phys. IV* **1** (1991) C3-495.
2. V. Q. HO and T. SUGANO, *IEEE Trans. Electron. Dev.* **ED 28** (1981) 1066.
3. R. F. WIELONSKI, P. J. MELLING and E. DRAUGLIS, in "29th Proceedings of the Annual Technical Conference of the Society of Vacuum Coaters", LA (Soc. Voc. Coaters, LA, 1986) pp. 254-61.
4. R. F. WIELONSKI and P. J. MELLING, US Pat. 470 4299A (1987).
5. L. MASCIA and Z. ZHANG, *J. Mater. Sci. Lett.* **14** (1995) 1199.
6. G. W. SCHERER, *J. Am. Ceram. Soc.* **60** (1977) 239.
7. H. DISLICH, in "Sol-Gel Technology For Thin Films, Fibers, Preforms, Electronics, and Speciality Shapes", edited by L. C. Klein (Noyes, NJ, 1988) p. 50.
8. K. KOHNO, *J. Mater. Sci.* **27** (1992) 658.
9. H. A. MACLEOD, "Thin-film Optical Filters" (Adam Hilger, Bristol, 1986).
10. B. Y. YOLDAS, *Appl. Optics* **19** (1980) 1425.
11. C. G. PANTANO, R. K. BROW and L. A. CARMAN, in "Sol-Gel Technology For Thin Films, Fibers, Preforms, Electronics, and Speciality Shapes", edited by L. C. Klein (Noyes, NJ, 1988) p. 110.
12. C. G. PANTANO, P. M. GLASER and D. J. ARMBRUST, in "Ultrastructure Processing of Ceramics, Glasses, and Composites", edited by L. L. Hench and D. R. Ulrich (Wiley, Canada, 1984) p. 161.
13. L. I. POPOVA, E. D. ATANASSOVA, S. K. PENEVA and E. A. TCUKEVA, *Cryst. Res. Techn.* **23** (1988) 979.
14. L. I. POPOVA, E. D. ATANASSOVA, S. K. PENEVA and E. A. TCUKEVA, *Mater. Lett.* **8** (1989) 357.
15. L. MASCIA and Z. ZHANG, *Appl. Surf. Sci.* **93** (1997) 1.

Received 18 December 1995

and accepted 2 July 1996